UCRL-91781
PREPRINT

ANALYSIS OF THE NAEG MODEL OF TRANSURANIC RADIONUCLIDE TRANSPORT AND DOSE

J.R. Kercher
L.R. Anspaugh

This paper was prepared for submittal to
Proceedings of the Nevada Applied Ecology Group
Information Meeting
Las Vegas, NV, June 28-30, 1983

November 1984

Lawrence Livermore National Laboratory

ABSTRACT*

We analyze the model for estimating the dose from ^{239}Pu developed for the Nevada Applied Ecology Group (NAEG) by using sensitivity analysis and uncertainty analysis. Sensitivity analysis results suggest that the air pathway is the critical pathway for the organs receiving the highest dose. Soil concentration and the factors controlling air concentration are the most important parameters. The only organ whose dose is sensitive to parameters in the ingestion pathway is the GI tract. The air pathway accounts for 100% of the dose to lung, upper respiratory tract, and thoracic lymph nodes; and 95% of the dose to liver, bone, kidney, and total body. The GI tract received 99% of its dose via ingestion. Leafy vegetable ingestion accounts for 70% of the dose from the ingestion pathway regardless of organ, peeled vegetables 20%; accidental soil ingestion 5%; ingestion of beef liver 4%; beef muscle 1%. Only a handful of model parameters control the dose for any one organ. The number of important parameters is usually less than 10.

Uncertainty analysis indicates that choosing a uniform distribution for the input parameters produces a lognormal distribution of the dose. The ratio of the square root of the variance to the mean is three times greater for the doses than it is for the individual parameters. As found by the sensitivity analysis, the uncertainty analysis suggests that only a few parameters control the dose for each organ. All organs have similar distributions and variance to mean ratios except for the lymph modes.

---

* Work performed under the auspices of the U.S. Department of Energy by the Lawrence Livermore National Laboratory under contract number W-7405-ENG-48.

INTRODUCTION

An important problem in assessing health risks from radionuclides has been the accurate quantification of transport from the source repository (soil) to the target organs of man through all the possible pathways. This quantification effort requires a two-part task. One part is a measurement program consisting of field and laboratory studies designed to gather data on all the various subprocesses. The second part is to cast these measurements into a simulation model of transport and dose. The model can act both as a research tool and as an assessment tool. As a research tool, the model stores and integrates the information from many different field and laboratory investigators. Because of the model, missing data become apparent. As an assessment tool, the model can be used to make estimations for various scenarios regarding contamination level, environment, lifestyles of people, etc. To be utilized fully in both the research management and the assessment roles, it should be recognized that the model contains much useful information other than single endpoint predictions of a particular set of scenarios. Sensitivity analyses and uncertainty analyses are two tools which we will use to explore a specific transuranic radionuclide transport and dose model.

Martin et al. (1974) developed a preliminary model of plutonium transport and dose for the Nevada Applied Ecology Group (NAEG) with the stated goal and assumptions as follows:

> "A preliminary model of potential plutonium transport to man was introduced during the planning stage of the NAEG Plutonium Study in an effort to ensure the inclusion of laboratory and field studies which would provide the data and parameter estimates needed for later implementation of a plutonium transport and dose estimation model

which would: (1) simulate the behavior of ^{239}Pu in desert ecosystems such as those found at the Nevada Test Site (NTS); (2) provide estimates of ^{239}Pu ingestion and inhalation rates by Standard Man, assumed to live in a ^{239}Pu-contaminated area; and (3) provide estimates of potential radiation doses, as a function of exposure time, to different organs."

This effort was in support of a general purpose of the NAEG Plutonium Study which was

". . . to evaluate the radiological hazards associated with plutonium-contaminated areas at the NTS and to recommend practical measures which could be taken, if necessary, to minimize such hazards now or in the future."

Modified and improved versions of this model were developed (Martin and Bloom, 1976, 1977). The improvements were the adoption of an improved inhalation model for man and simplifications in the vegetation-concentration portions of the model. Using the ingestion submodel for grazing cattle, Martin and Bloom (1978a) analyzed the results of field studies at NTS and found good agreement between model and experiment. They concluded that the experiments were internally consistent and well designed. Martin and Bloom (1977, 1980) also made detailed comparisons between NAEG model versions which had the International Commission on Radiological Protection (ICRP) II lung model (ICRP, 1959), the ICRP Task Group on Lung Dynamics (ICRP, 1972) lung model, and a lung model proposed by Stuart et al. (1968, 1971). Martin and Bloom (1980) concluded that the model of the ICRP Task Group on Lung Dynamics was the model of choice. Martin and Bloom (1978b) considered the effects of variations in model parameters on model results and examined the variations among predicted results for the three translocation classes that can be

assigned to ^{239}Pu, i.e., daily, weekly, or yearly (ICRP, 1972). They also considered the effect of particle size (activity median aerodynamic diameter, AMAD) on equilibrium-lung burden and the rate at which ^{239}Pu reaches the blood. They also examined bone burden as a function of blood-to-bone transfer rates and turnover time in bone. However, Martin and Bloom (1978b) did not provide a comprehensive sensitivity analysis of the effect of variation of all model parameters on the cumulative dose to all target organs. We will examine the sensitivity of the NAEG model in this work. In addition, we will analyze the contribution of each pathway to the dose of each organ, and we will discuss the uncertainty in the model's predicted results based upon simultaneous propagation of all model parameters.

NAEG MODEL DESCRIPTION

The model has been fully described by Martin and Bloom (1980), so we will here give only a brief synopsis of the basic approach and equations. The model can be generalized to all important radionuclides which occur at NTS, but in the present form the model only addresses the problem of ^{239}Pu in the yearly translocation class. It is designed with the assumption that a Reference Man (ICRP, 1975) is living in a contaminated environment, eating only plants and animals living in the same environment. Thus, given a contaminated substrate, the model assumes maximum exposure to that environment. (With modification, the model could be used to evaluate only partial exposure to the contaminated environment or to contaminated foodstuffs.)

The model divides the system into these compartments: (1) soil, (2) desert vegetation, (3) cultivated vegetables, (4) alfalfa, (5) beef cattle, (6) milk cows, (7) air, and (8) man (see Fig. 1). The beef cattle, milk cow, and man

submodels describe radionuclide movement between internal organs. The transfers between the compartments are linear functions of the amount of radionuclide in the donor compartment. Thus the model is described as a set of linear, ordinary, donor-controlled differential equations. The ecosystem portion of the model is not treated as fully dynamic. That is, the air, vegetation, and milk-cow compartment equations are solved at steady-state. The beef cattle equations are solved at a fixed endpoint, i.e., time-of-slaughter. Thus, the ecosystem portion of the model is static. The man model (ICRP, 1972), on the other hand, is fully dynamic, i.e., the compartment burdens and dose rates change over time.

TOTAL SYSTEM

There are direct transfers from soil to all three types of vegetation primarily through an external mechanism (Fig. 1). Martin and Bloom (1977) citing Romney et al. (1975) concluded that root uptake constitutes "no more than 1% of Pu in plant samples from contaminated areas at NTS." There are transfers from the three vegetation compartments to man, beef cattle, and milk cows reflecting ingestion of plants. There is also a direct transfer from soil to the GI submodels of man, which reflects the accidental ingestion of soil particles. Grazing cattle also ingest soil along with vegetation. Hence, there are direct transfers from the soil to both the beef cattle and milk-cow compartments. In addition to vegetation, man also ingests beef muscle, beef liver, and cow's milk. There is also an inhalation pathway through an atmospheric compartment via the resuspension mechanism. A strong modifying variable is the fractional distribution of the radionuclide among particle size classes. This is discussed in detail below.

AIR CONCENTRATION

The concentration of Pu in air C_a (pCi/m^3) is modeled from the mass-loading approach. That is

$$C_a = L_a C_s \tag{1}$$

where C_s is the concentration of Pu in soil (pCi/g soil) and L_a is a mass-loading factor of soil particles in air (g soil/m^3 air). See Table 1 for parameter value of L_a.

PLANT CONCENTRATION

The NAEG model uses the concentration factor approach for calculating y_v, the concentration of Pu in plant tissue (pCi/g). In the NAEG model, all plant and animal tissue concentrations are on a dry weight basis. Conceptually, the plant is considered to be one compartment with an uptake rate and a loss rate dependent on body burden, i.e.,

$$\frac{dy_v}{dt} = U_p - L_o y_v \tag{2a}$$

where U_p is an uptake rate (pCi/g-day) and L_o is a turnover rate (day^{-1}). The uptake rate is a transfer from soil to plant and is assumed to be proportional to C_s,

$$U_p = uC_s \ , \tag{2b}$$

with proportionality constant u (day^{-1}). At steady state, Eq. 2a becomes

$$y_v = \frac{u}{L_o} C_s = CF_v C_s \tag{3}$$

where CF_v is the concentration factor for vegetation (dimensionless). Note the similarity between Eq. 1 and Eq. 3. Equation 2a is a linear, donor-controlled ordinary differential equation. The parameters of Eq. 3 are shown in Table 1.

BEEF-CATTLE SUBMODEL

In Fig. 2, we show the schematic for the beef-cattle submodel. The accumulation of Pu in cattle is estimated to be dominated by ingestion. There are two ingestion pathways, accidental soil ingestion I_s (g/day) and vegetation ingestion I_v (g/day). I_v is calculated from the empirical formula for the energy needs of cattle,

$$W = CF_1 \, (WBEEF)^{CF_2} , \tag{4}$$

divided by the energy content of vegetation. Thus,

$$I_v = \frac{CF_1 \, (WBEEF)^{CF_2}}{DIG \cdot PLE} \tag{5}$$

where W is the digestible energy required per day for maintenance for cattle of size WBEEF; CF_1 and CF_2 are empirical constants (Siegmund, 1967); DIG is the fraction of energy of desert vegetation which is digestible; PLE is the energy content of desert vegetation (kcal/g).

Inside the animal, the fractional amount of Pu that transfers from gut to blood is given by f_{bgi}. The fraction transferring from blood to muscle is f_{msb} and the portion transferring from blood to liver is f_{livb}. The turnover rate in muscle is λ_{ms} and the turnover rate in beef liver is λ_{lv}. Thus the differential equations for the total burden of Pu in beef muscle y_{ms} (pCi) and beef liver y_{liv} (pCi) are

$$\frac{dy_{ms}}{dt} = C_s\,(CF_vI_v + I_s)f_{bgi}f_{msb} - \lambda_{ms}y_{ms} \qquad (6a)$$

and

$$\frac{dy_{liv}}{dt} = C_s\,(CF_vI_v + I_s)f_{bgi}f_{livb} - \lambda_{lv}y_{liv}. \qquad (6b)$$

These equations can be turned into concentration equations by dividing them by the mass of beef muscle (m_{ms}) and mass of beef liver (m_{liv}), respectively. The solutions for the concentrations, C_{muscle} and C_{liver} (pCi/g) are

$$C_{muscle} = \frac{C_s\,(CF_vI_v + I_s)f_{bgi}f_{msb}}{m_{ms}\lambda_{ms}}\,(1 - e^{-\lambda_{ms}t}) \qquad (7a)$$

and

$$C_{liver} = \frac{C_s\,(CF_vI_v + I_s)\,f_{bgi}f_{livb}}{m_{liv}\lambda_{lv}}\,(1 - e^{-\lambda_{lv}t}) \qquad (7b)$$

where turnover rates are given by

$$\lambda_{lv} = \ln(2)/T_{liv} \text{ and } \lambda_{ms} = \ln(2)/T_{ms} \qquad (7c)$$

and where T_i is the biological half time of Pu in compartment i. At the time of slaughter t has the value Time. Values for the parameters in Eqs. 4 through 7 are given in Table 2.

MILK-COW SUBMODEL

The milk-cow submodel is shown in Fig. 3. It is very similar to the beef-cattle submodel except that the transfer is to the milk compartment. Also,

lactating cows require nourishment in addition to the maintenance requirement expressed in Eq. 4. Assuming this is supplied by a cultivated plant such as alfalfa, we replace Eq. 5 by

$$I_v = I_{vd} + I_{va} = \frac{CF_1(WMILK)^{CF_2}}{DIG \cdot PLE} + \frac{FAC \cdot PMILK}{DIG_A \cdot PLE} \quad (8)$$

where WMILK is the weight of the cow (kg), DIG_A is the digestibility factor for alfalfa, PMILK is the daily production of milk (kg/day), and FAC is the energy required to produce 1 kg of milk (kcal/kg). Using this expression for I_v in Eq. 7a and replacing f_{msb} by f_{milkb}, we can derive an expression similar to Eq. 7a. However, the residence time for milk, $1/\lambda_{milk}$, is so short that the exponential term is very small compared to one for any realistic t. Therefore the resulting milk concentration equation is solved at steady state to give

$$C_{milk} = \frac{(I_{vd} + I_{va}/F_{alf})CF_v + I_s}{P_{milkg}\,\lambda_{milk}}\; C_s f_{bgi} f_{milkb} \quad (9)$$

where

$$\lambda_{milk} = \ln(2)/T_{milk}$$

and P_{milkg} is the daily production of milk in grams, F_{alf} is a factor reducing the concentration in alfalfa to account for the soil mixing by cultivation in cultivated crops and T_{milk} is the biological half time of milk in the cow. The NAEG model assumes that Pu is concentrated in the top 5 cm in desert soils at the NTS. In cultivated soil, this top layer is mixed to a greater depth by

plowing, discing, etc. For the NAEG model, the greater cultivation depth is taken to be 30 cm, which means F_{alf} is equal to 6. Parameters for Eqs. 4 through 9 are in Table 3.

MAN SUBMODEL

We show a compartment diagram of the man submodel in Fig. 4. Martin and Bloom (1980) ultimately decided on the formulation proposed by the ICRP Task Group on Lung Dynamics for the lung portion of the man submodel. This has since been adopted as ICRP 19 (ICRP, 1972) and ICRP 30 (ICRP, 1979). We have used the parameter set of Martin and Bloom (1980) for comparison of our results with theirs. This parameter set differs slightly from ICRP 19. Note that in the structure of the model there are two possible inputs: respiration and ingestion. Material taken into the lung or GI tract (gut) can cross into the blood compartment and be transferred to the various body organs. Obviously the transfer coefficients are important in determining the distribution throughout the body. In the analysis to follow, we can estimate the relative importance between the various coefficients.

Inhalation and Lung Model

The rate of inhalation of Pu into man A_m (pCi/day) is given by

$$A_m = B_m L_a C_s \qquad (10)$$

where B_m is the respiration rate (m^3/day). The Pu is carried on particles and the particles are distributed over various size classes of activity median aerodynamic diameter (AMAD). Martin and Bloom (1980) implemented ICRP 19 with

seven AMAD size classes (0.05, 0.1, 0.3, 0.5, 1.0, 2.0, 5.0 μm) and there is a fraction FR_i in the ith size class. For the ith size class particles, the fraction $D_{3,i}$ is deposited in the nasopharyngel region, the fraction $D_{4,i}$ is deposited in the tracheobronchial region, and the fraction $D_{5,i}$ is deposited into the lung. Of the Pu deposited in the nasopharyngeal region, the fraction f_a is cleared to the blood with the transfer rate λ_a and f_b is cleared to the GI tract (or gut) with transfer rate λ_b. Of the Pu deposited in the tracheobronchial region, the fraction f_c is transferred to the blood with a transfer rate of λ_c and the fraction f_d is cleared to the GI tract with a transfer rate of λ_d. Of the Pu deposited in the lung, the fractions f_f and f_g are cleared to the GI tract through the tracheobronchial region with transfer rates λ_f and λ_g, respectively. The transit time in the tracheobronchial region is $T_{TBf,g}$. The fraction f_e of Pu deposited in the lung is cleared to the blood with transfer rate λ_e and the fraction f_h is cleared to lymph nodes with transfer rate λ_h. Of the Pu deposited in the lymph nodes, the fraction f_i is cleared to blood with transfer rate λ_i. The remaining fraction $(1 - f_i)$ remains in the lymph nodes. So the mass balance equations for the lung model are as follows:

Let $$D_3 = \sum_{i=1}^{7} FR_i D_{3,i} \qquad (11a)$$

$$D_4 = \sum_{i=1}^{7} FR_i D_{4,i} \qquad (11b)$$

$$D_5 = \sum_{i=1}^{7} FR_i D_{5,i} \qquad (11c)$$

Then

$$\frac{dy_{NPa}}{dt} = f_a D_3 A_m - (\lambda_A + \lambda_a)\, y_{NPa} \qquad (12a)$$

$$\frac{dy_{NPb}}{dt} = f_b D_3 A_m - (\lambda_A + \lambda_b)\, y_{NPb} \tag{12b}$$

$$y_{NP} = y_{NPa} + y_{NPb} \tag{13}$$

$$\frac{dy_{TBc}}{dt} = f_c D_4 A_m - (\lambda_A + \lambda_c)\, y_{TBc} \tag{14a}$$

$$\frac{dy_{TBd}}{dt} = f_d D_4 A_m - (\lambda_A + \lambda_d)\, y_{TBd} \tag{14b}$$

$$\frac{dy_{Pe}}{dt} = f_e D_5 A_m - (\lambda_A + \lambda_e)\, y_{Pe} \tag{15a}$$

$$\frac{dy_{Pf}}{dt} = f_f D_5 A_m - (\lambda_A + \lambda_f)\, y_{Pf} \tag{15b}$$

$$\frac{dy_{Pg}}{dt} = f_g D_5 A_m - (\lambda_A + \lambda_g)\, y_{Pg} \tag{15c}$$

$$\frac{dy_{Ph}}{dt} = f_h D_5 A_m - (\lambda_A + \lambda_h)\, y_{Ph} \tag{15d}$$

$$y_{TBf,g} = (\lambda_f y_{Pf} + \lambda_g y_{Pg})\, T_{TBf,g} \tag{16a}$$

$$y_{TB} = y_{TBc} + y_{TBd} + y_{TBf,g} \tag{16b}$$

$$y_P = y_{Pe} + y_{Pf} + y_{Pg} + y_{Ph} \tag{17}$$

$$\frac{dy_{LMi}}{dt} = f_i \lambda_h y_{Ph} - (\lambda_A + \lambda_i)\, y_{LMi} \tag{18b}$$

$$\frac{dy_{LMj}}{dt} = (1 - f_i)\, \lambda_h y_{Ph} - \lambda_A y_{LMj} \tag{18b}$$

$$y_{LM} = y_{LMi} + y_{LMj} \tag{19a}$$

where the subscripts NP refer to nasopharyngeal, TB refers to tracheobronchial, P refers to pulmonary (lung), and LM refers to lymph nodes. The total body burden for these organs are the sums across the subcompartments as in Eqs. 13, 16b, 17, and 19a, respectively. Each transfer rate is given by

$$\lambda_l = \ln(2)/T_l^b \tag{19b}$$

where T_l^b is the biological half time for compartment l, except λ_A is the physical decay rate of ^{239}Pu. Table 4 contains the values of the lung model parameters, Eq. 10 through 19.

Ingestion By Man

The total ingestion rate H_m (pCi/day) shown in Fig. 4 is given by

$$H_m = C_s \sum_{i=1}^{6} I_i \, Disc(i) \tag{20a}$$

where i represents one of the six ingestion pathways explained in Table 5, I_i is the amount ingested via pathway i (g/day), and Disc(i) is the discrimination ratio for food type i. The discrimination ratio is defined as the ratio of the concentration of Pu in the food to that in soil.

That is

$$Disc(1) = 1 \tag{20b}$$

$$Disc(2) = Wash \cdot CF_v/F_{alf} \tag{20c}$$

$$Disc(3) = Peel \cdot CF_v/F_{alf} \quad (20d)$$

$$Disc(4) = C_{muscle}\ (Time)/C_s \quad (20e)$$

$$Disc(5) = C_{liver}\ (Time)/C_s \quad (20f)$$

$$Disc(6) = C_{milk}/C_s \quad (20g)$$

where Time is the value of t in Eq. 7a and 7b when the animal is slaughtered. Table 5 contains the values and descriptions of parameters in Eq. 20.

Submodel for Distribution in Man

The transfer into the gut is

$$r_{GIT} = \lambda_b y_{NPb} + \lambda_d y_{TBd} + \lambda_f y_{Pf} + \lambda_g y_{Pg} + H_m \quad (21)$$

Because the residence time in the gut is so short compared to that of the simulation times, we can use an argument similar to that of milk for the milk cow and arrive at an equation for the burden in the gut.

$$y_{GIT} = r_{GIT}\ T_{GIT} \quad (22)$$

where T_{GIT} is the residence time in the gut. The transfer rate into the blood is

$$r_B = \lambda_a y_{NPa} + \lambda_c y_{TBc} + \lambda_e y_{Pe} + \lambda_i y_{LMi} + f_j r_{GIT} \quad (23)$$

The equations for liver, kidney, bone, and total body are

$$\frac{dy_{liv}}{dt} = f_{BL} r_B - (\lambda_A + \lambda_L) y_{liv} \quad (24)$$

$$\frac{dy_{kid}}{dt} = f_{BK} r_B - (\lambda_A + \lambda_K) y_{kid} \quad (25)$$

$$\frac{dy_{bone}}{dt} = f_{BBN} r_B - (\lambda_A + \lambda_{BN}) y_{bone} \quad (26)$$

$$\frac{dy_{totb}}{dt} = f_{BTB} r_B - (\lambda_A + \lambda_{TOTB}) y_{totb} \quad (27)$$

See ICRP 19 for a full discussion of the man submodel. The definitions of the λ's are

$$\lambda_x = \ln 2 / T_x \quad (28)$$

where x is L, BN, K, and TOTB. The parameters for Eqs. 21 through 28 are given in Table 6.

Dose to Man

The time rate of change of the dose D_s (rem) to a target organ, s, is given by

$$\frac{dD_s}{dt} = \frac{E_s}{m_s} y_s \quad (29)$$

where

$E_s = 51.2159 \times 10^{-6} \epsilon_s$, dose rate factor, (g rem pC_i^{-1} day^{-1})

ϵ_s = effective energy absorbed in the organ s per disintegration of radionuclide (MeV/dis)

m_s = mass of target organ s except for GI dose in which case it equals twice mass of contents of GI tract.

The organs for which we calculated a dose are liver, kidney, bone, total body, upper respiratory tract, GI tract, lungs, and thoracic lymph nodes. The doses for liver, kidney, bone and total body were calculated using the y's or body burdens of equations 24 through 27 respectively. The dose to the upper respiratory tract was calculated as

$$D_{URT} = \frac{E_{NP} \int_0^{T_D} y_{NP} dt + E_{TB} \int_0^{T_D} y_{TB} dt}{m_{NP} + m_{TB}} \qquad (30)$$

where y_{NP} is from Eq. 13 and y_{TB} is from Eq. 16b. The calculation for dose to the lung, lymph, and GI tract uses y_p from Eq. 17, y_{LM} from Eq. 19, and y_{GIT} from Eq. 22, respectively. Table 7 gives the parameters for the dose calculation. T_D is fifty years for the calculations in this paper.

RESULTS OF SIMULATION

We ran a 50-year simulation assuming a constant value for C_s of 1.0 pCi/g. Equations 1 through 11 are solved algebraically. Equations 12 through 30 are solved with the eigenvalue-eigenvector method using a code developed by Reeves (1971). In Figure 5, we show the doses as a function of time for lung, gut, bone, and liver. Because both the lung and gut have relatively rapid turnover rates, their contents reach a steady state soon after the simulation begins. Thereafter their doses rise linearly as the dose becomes proportional with time in the integral of Eq. 29. However, since both the liver and the bone have long residence times, their contents do not equilibrate during the simulation but instead increase monotonically. Therefore, their doses seen in Fig. 5 rise faster than linearly. Note that the dose to the GI tract is two orders of magnitude less than the other three. This can be seen more clearly in Fig. 6

where all the doses are plotted on the same graph on logarithmic scales. There we see that the lung, bone, and liver are the critical organs. The thoracic lymph nodes have the highest dose but since there is not a generally accepted interpretation of dose to the thoracic lymph nodes, we will concentrate on the other organs in our analysis.

Based on similar results which they found, Martin and Bloom (1980) calculated an acceptable soil concentration (ASC). Using the lung as the critical organ which would have a permissible dose rate of 1.5 rem/year, they calculated that the corresponding soil contamination level would be 2817 pCi ^{239}Pu/g soil.

SENSITIVITY ANALYSIS

METHODOLOGY

The sensitivity analysis was done by looking at the 50-year dose for each of the eight organs listed shown in Fig. 6. To calculate the sensitivity of each of these doses to any one parameter, say parameter i, we hold all other parameters at their nominal values and increase parameter i by 10%. The doses must be calculated both at the nominal value of a_i and at the new value of a_i. Then the sensitivity $\Gamma_{j,i}$ of the dose to the jth organ to a change in parameter a_i is given by

$$\Gamma_{j,i} = \frac{\dfrac{\text{Dose}_j(50y,\ a_{i\ new}) - \text{Dose}_j(50y,\ a_{i\ old})}{\text{Dose}_j(50y,\ a_{i\ old})}}{\dfrac{a_{i\ new} - a_{i\ old}}{a_{i\ old}}} \qquad (31)$$

where "old" designates the nominal value of the ith parameter and "new" designates the new value or 1.1 times the old value. Note that the sensitivity is a fractional change in the dose per fractional change in the parameter. Thus, for Γ equal to about 1, we would consider an organ dose to be sensitive to that parameter or in shorthand we would refer to the parameter as a sensitive parameter. This is because a one part change in the parameter is producing a one part change in the dose. For Γ equal to about 0.1 or less, we would refer the dose as being insensitive to that parameter or colloquially we would refer to the parameter as "insensitive." This is because a one part change in the parameter produces only a 1/10 part change in the dose. We also note that Eq. 31 can be simplified to

$$\Gamma_{j,i} = 10 \frac{\text{Dose}_j(50y,\ 1.1a_i) - \text{Dose}_j(50y,\ a_i)}{\text{Dose}_j(50y,\ a_i)} \qquad (32)$$

RESULTS OF SENSITIVITY ANALYSIS

We will examine in detail the results of the sensitivity analysis for dose to the lung, bone, liver, and GI tract. The first three organs were chosen because they receive the largest dose (excluding the lymph nodes for which there is no accepted interpretation for dose). The GI tract was chosen because of its unique status in the model and also for the eventual comparison of these results to other radionuclides for which the GI tract might receive a significantly larger dose. In addition to the detailed examination of specific organs, we will also compare the pathways using sensitivity analysis.

Organ Analysis

In Table 8 we show the sensitivity results for the lung dose. In Table 8, the first three parameters determine the intake of Pu to the lung and the fourth is a multiplicative factor determining the dose from the body burden. Because the mass of the lung is a divisor in the equation for dose, a 10% increase in the mass results in a 9.1% decrease in the dose. The next nine parameters are in the lung model and determine the quantity of Pu deposited and retained in the deep pulmonary tissues, residence times, and clearance rates from pulmonary tissues. These nine lung-model parameters span the sensitivity range from 0.67 down to 0.14. Then there are 14 nonzero parameters in the sensitivity range 0.11 down to 0.0. These are all lung-model parameters of a physiological nature or parameters having to do with the distribution of Pu among particle sizes. Then there are 83 other parameters in the model having to do with the food chain or other organs in man for which the lung dose has zero sensitivity.

In Table 9 we show the sensitivity of the bone dose to parameter changes. Three parameters have a sensitivity of 1.0. That is, the dose is directly proportional to the concentration of Pu in the soil, the transfer coefficient of blood to bone, and the dose factor for bone. The next two parameters, mass loading factor for air and the respiration rate for man, have a sensitivity of 0.95. This is because 95% of the dose to bone comes from the air or inhalation pathway rather than the food or ingestion pathway. After the mass of bone come seven lung-model parameters having to do with the fractions of Pu cleared to blood and lymph (f_h, f_i, f_e), retention factors for various size classes (D_5's) in the lung, and the portion of Pu particles in the 0.05μ size class. These sensitivities range between 0.62 and 0.11. There are 58 parameters of the model with a sensitivity between 0.1 and 0.00002. There are 14 nonzero

parameters with a value less than 0.5×10^{-5}. There are 25 parameters with a sensitivity of 0.0. In particular, note the sensitivities for parameters I_1 through I_6. Their extremely small size indicates the relative unimportance of the ingestion pathway for "year-class" Pu in this environment. The relatively large sensitivity of leafy vegetable ingestion compared to beef-product ingestion is due in part to the small transfer coefficient in the animal from gut to the blood. Also note the relatively larger sensitivity of liver ingestion over muscle ingestion. This is because the accumulated levels in the liver are significantly greater than those in muscle.

In Table 10 we show the sensitivity of the liver dose to changes in model parameters. Comparing Tables 9 and 10, we see that they are almost identical. The only difference is that the residence time of Pu in the liver is present in Table 10 but not in Table 9. This is to be expected. The reason for the similarities between Tables 9 and 10 become clear if we look at the diagram for the man model, Fig. 4. There it is apparent that both the liver and bone receive their Pu from the same compartment, the blood. Thus, any change in the model parameters, which come before blood compartment in the Pu stream, will produce the same change in the intake to both the liver and kidney compartments. So when considering the structure of the model, the bone and liver compartments are very similar.

Looking at Fig. 4, we see that the gut compartment is unique. This is reflected in Table 11. We see that the concentration in the soil, residence time in the GI tract, and the dose-rate factor are all proportional to the dose. The concentration factor for vegetation sums the contributions of man's direct ingestion of washed and peeled vegetables and the Pu which man receives from beef products which the cattle in turn had acquired from vegetation. The remaining 7% contribution of dose to gut comes from accidental ingestion of soil by man and animals and the inhalation pathway. Note that the soil-mixing-

by-cultivation factor F_{alf} ranks relatively high. This suggests that environmental manipulation could reduce this dose. Ingestion of leafy (washed) vegetables contributes 70% of the dose and ingestion of other (peeled) vegetables contributes 19%. The parameter CF_2 ranks higher than the other cattle parameters because it is an exponent in the cattle-feed ingestion equation. Thus, a relatively small change in this parameter produces a relatively larger change than other parameters in the same equation. We see that accidental ingestion of soil by man still ranks higher than eating beef products in dose sensitivity. However, the sum total for beef products contribution to dose (5%) is higher for the gut compartment than for any other. The fact that the transfer coefficient from gut to blood acts like a very strong filter produced the result that ingestion was not important for the liver and bone compartments.

Pathway Analysis

Table 12 shows the sensitivity-analysis results grouped in such a way that the pathway contributions to the dose are displayed. For example, the upper respiratory tract, lung, and thoracic lymph nodes receive 100% of their dose from the inhalation pathway. The liver, kidney, bone, and total body receive 95% of their dose from the inhalation pathway. Note that the column sums for the inhalation pathway plus either of the breakdowns of the ingestion pathway are 100% for each organ. The ingestion pathway contribution for all organs is dominated by the intake from leafy vegetables. The contribution to dose from beef products is miniscule for all organs except the gut, where it is 5%. Ultimately, 93% of the ingestion-pathway contribution to dose comes through vegetation and 7% comes through accidental soil ingestion either by cattle or

by man. The only organ that receives a substantial fraction of its dose from the ingestion pathway is the GI tract. It receives 99.4% of its dose from ingestion and only 0.6% of its dose from inhalation.

UNCERTAINTY ANALYSIS

There is an intrinsic uncertainty associated with each parameter in the NAEG model. This uncertainty can reflect measurement error or an intrinsic variability in the parameter. For example, biological parameters often vary over a wide range because of genetic variability within a population. Thus, a parameter may be very accurately measured for one individual and yet be quite different from the same accurately measured parameter for another individual. The question arises then as to how much variability there is in the final result of the NAEG model dose calculations for the entire set of input parameters, when each one has some uncertainty associated with it and all can simultaneously be quite different from their nominal averages.

PROCEDURE

We use what is known as the "Monte Carlo" approach in carrying out the uncertainty analysis. We let each parameter vary independently. In general, for each run of the model, we pick a random number for each variable from the uncertainty distribution for that variable. In the analysis presented here, we will use a uniform distribution for each variable with a ±5% range around the mean. That is, we assume that for a specific run, the value of each variable is within 5% of the mean value for that variable and that any value is as likely to be chosen as any other value within that ±5% spread. This

exercise will give us an indication of what to expect if distributions based on real field data were used to generate the uncertainty distributions. Using this basic procedure, we ran the model 1000 times and examined the resulting distributions for the 50-year doses.

RESULTS

The uncertainty analysis generates a considerable amount of data on the distribution of dose. We will use exploratory analysis techniques to analyze these results (Axelrod, 1978). In Fig. 7, we show histograms of the distributions of 50-year doses for the four compartments: lung, liver, bone, and gut. Note that selecting parameters from uniform distributions resulted in non-uniform distributions for the resulting doses. That is, we produced double-tailed distributions that have the appearance of distributions one might observe from field measurements. The doses are very slightly skewed to the high end. This is not evident from Fig. 7. But if the doses for a given organ, D_i, are sorted by value with i running from 1 to N, and the value of $(D_{median}-D_i)$ is plotted against $(D_{N-i+1} - D_{median})$, we found that the distributions in Fig. 7 are skewed to the high end. The spread in the distributions of the organ doses is greater than the spread in the individual parameters. This is evident in Fig. 7. In Table 13 we show the square root of the variance divided by the mean for a typical parameter and for each of the organ doses. We see that all the compartments have similar spreads except the thoracic lymph node compartment. This result indicates that an analysis based solely on the sensitivity analysis would not give a complete picture of the variation in the model. That is, to predict model-output variation, one cannot rely solely on sensitivity analysis since in this case we produced a variation greater than the spread of any one parameter. The lymph-node

compartment is unique in that it is the only one which does not have a transfer out. Possibly this property is the cause of the larger variance in the dose. For all the other compartments we see that the spread is three times that of the spread of each individual parameter. This indicates that only a relatively few parameters are important in determining the dose. This result agrees with the outcome of the sensitivity analysis.

In Fig. 8 we plot the same data against the probit or normal quantile scale after having taken the log of the data, i.e., log probability plots. The data for all four of these organ doses seem to fall along a straight line. This suggests that the distributions of Fig. 7 are best represented as lognormal distributions. (The logarithm of the dose is normally distributed.) In comparison, we plot the untransformed data on probability plots in Fig. 9. Here the data deviate more from a straight line. It should be pointed out that this effect is small because our assumed spread in the input parameters is so small (±5%). For larger variances for model parameters similar to the variance experienced in field measurements, we would see a much larger variance in the organ doses. This would be reflected in much larger distinctions between untransformed and log transformed data.

CONCLUSIONS

We have performed an analysis of the NAEG model by using sensitivity analysis and uncertainty analysis.

The sensitivity analysis indicates that the air pathway is the critical pathway for the organs receiving the highest dose (critical organs). The soil concentration and the factors controlling air concentration are the most

important parameters. The only organ dose sensitive to parameters in the ingestion pathway is the GI tract. The air pathway accounts for 100% of the dose to lung, upper respiratory tract and thoracic lymph nodes from Pu; 95% of the dose to liver, bone, kidney, and total body. On the other hand, the GI tract receives 99% of its dose via ingestion. The GI tract dose is sensitive to these environmental parameters: concentration in soil, concentration factors for plants, depth of plowing, and Pu retained on leafy vegetables after washing.

The uncertainty analysis indicates that choosing a square or uniform distribution for the input parameters results in a lognormal distribution of dose. The ratio of the square root of the variance to the mean is three times greater for the doses than it is for the individual parameters. Thus, only a few parameters control the dose for each organ. All organs have similar distributions and variance to mean ratios except for the lymph nodes.

These results suggest that expenditure of future effort should be in the improvement of the air-pathway submodel. It would also be useful to incorporate realistic distributions of parameters in the uncertainty analysis. The choice for which parameters should be extracted from existing data bases or from literature searches should be based on the sensitivity-analysis results. While we anticipate that the lognormal result is sufficiently robust that it will be found to be true when realistic data are used in the uncertainty analysis, the predicted dose distribution made from actual data would be extremely valuable in evaluating the radiological hazard from Pu.

If the goals of the NAEG model program are broadened from a focus on research on Pu movement to an emphasis on radiological hazard, then other radionuclides should be incorporated in the model as identified by the Radionuclide Inventory and Distribution Project to evaluate better the true

radiological hazard. If other radionuclides are added, then in addition to the pathways currently in the NAEG model, an external dose should also be calculated for all the gamma-emitting radionuclides of concern. If a fuller, more complicated model is developed along these lines, then the sensitivity and uncertainty analyses should be repeated to understand better the implications of the expanded model.

REFERENCES

Axelrod, M.C. 1978. "An Exploratory Data Analysis of Photochemical Oxidants in the Imperial Valley, California." In: Electronics Engineering Department Quarterly Report No. 3-1978. Lawrence Livermore National Laboratory, Livermore, CA, UCRL-500025-78-3, pp. 25-34.

International Commission on Radiological Protection (ICRP). 1959. Recommendations Report of Committee II on Permissible Dose for Internal Radiation. ICRP Publication 2. Pergamon Press, New York.

International Commission on Radiological Protection (ICRP). 1972. The Metabolism of Compounds of Plutonium and Other Actinides. ICRP Publication 19, Pergamon Press, New York.

International Commission on Radiological Protection (ICRP). 1975. Report of the Task Group on Reference Man, ICRP Publication 23, Pergamon Press, New York.

International Commission on Radiological Protection (ICRP). 1979. Limits for Intakes of Radionuclides by Workers. ICRP Publication 30, Part 1, Pergamon Press, New York.

Martin, W.E., S.G. Bloom, and R.J. Yorde, Jr. 1974. "NAEG Plutonium Study Modeling Program: Plutonium Transport and Dose Estimation Model." In: The Dynamics of Plutonium in Desert Environments, Nevada Applied Ecology Group Progress Report as of January 1974, P.B. Dunaway and M.G. White, Eds., USDOE Report, NVO-142, pp. 331-360.

Martin, W.E. and S.G. Bloom. 1976. "Plutonium Transport and Dose Estimation Model." In: Transuranium Nuclides in the Environment, IAEA, Vienna, pp. 385-400.

Martin, W.E. and S.G. Bloom. 1977. "Nevada Applied Ecology Group Model for Estimating Plutonium Transport and Dose to Man." In: Transuranics in Natural Environments, M.G. White, and P.B. Dunaway, Eds., USDOE Report, NVO-178, pp. 621-706.

Martin, W.E. and S.G. Bloom. 1978a. "Simulation of Plutonium Ingestion by Grazing Cattle." In: Selected Environmental Plutonium Research Reports of the NAEG, M.G. White and P.B. Dunaway, Eds. USDOE Report, NVO-192, vol. 2 pp. 513-536.

Martin, W.E. and S.G. Bloom. 1978b. "The Effect of Variation in Source Term and Parameter Values on Estimates of Radiation Dose to Man." In: Selected Environmental Plutonium Research Reports of the NAEG, M.G. White and P.B. Dunaway, Eds. USDOE Report, NVO-192, vol. 2, pp. 483-512.

Martin, W.E. and S.G. Bloom. 1980. "Nevada Applied Ecology Group Model for Estimating Plutonium Transport and Dose to Man." In: Transuranic Elements in the Environment, W.C. Hanson, Ed., USDOE Report, DOE/TIC-22800, pp. 459-512.

Reeves, Mark, III. 1971. A Code for Linear Modeling of an Ecosystem. Oak Ridge National Laboratory, Oak Ridge, TN, ORNL-IBP-71/2.

Romney, E.M., A. Wallace, R.O. Gilbert, and J.E. Kinear. 1975. "239-240-Pu and 241-Am Contamination of Vegetation in Aged Plutonium Fallout Areas." In: The Radioecology of Plutonium and Other Transuranics in Desert Environments, M.G. White and P.B. Dunaway, Eds., USDOE Report, NVO-153, pp. 43-87.

Siegmund, O.H., Ed., 1967, The Merck Veterinary Manual, 3rd ed., Merck & Co., Inc., Rahway, NJ.

Stuart, B.W., P.J. Dionne, and W.J. Bair. 1968. "A Dynamic Simulation of the Retention and Translocation of Inhaled Plutonium Oxide in Beagle Dogs." In: Proceedings of the Eleventh AEC Air Cleaning Conference, M.W. First and J.M. Morgan, Jr., Eds., USAEC Report, CONF-700816.

Stuart, B.W., P.J. Dionne, and W.J. Bair. 1971. "Computer Simulation of the Retention and Translocation of Inhaled 239-PuO_2 in Beagle Dogs." In: Pacific Northwest Laboratory Annual Report for 1970 to the USAEC Division of Biology and Medicine, Vol. 1, Life Sciences, Pt. 1, Biological Sciences, Battelle, Pacific Northwest Laboratories, Richland, WA, BNWL-1550 (Pt. 1).

Table 1. Parameters and their values for the vegetation and air submodels.

Parameter or variable	Description	Value
C_a	Concentration of Pu in air (pCi/m^3)	
L_a	Mass loading of soil particles in air (g soil/m^3air)	0.0001
C_s	Concentration of Pu in soil (pCi/g)	1.0
CF_v	Concentration factor for vegetation (dimensionless)	0.1

Table 2. Parameters and their values for the beef-cattle submodel.

Parameter	Description	Value
CF_1	Energy requirement of cattle per unit body weight raised to the CF_2 power (kcal day^{-1} kg^{-CF_2})	163.5
CF_2	Exponent of body weight of cattle to calculate ingestion by cattle	0.73
WBEEF	Weight of beef cattle (kg)	275
DIG	Digestible fraction of desert vegetation	0.36
PLE	Energy content of vegetation (kcal/g)	4.5
f_{msb}	Fraction Pu transferred from blood to muscle	0.07
f_{bgi}	Fraction Pu transferred from gut to blood	3.0×10^{-5}
m_{ms}	Mass of muscle (g)	125×10^3
T_{ms}	Biological half time of Pu in beef (day)	2000
I_s	Accidental ingestion rate of soil (g/day)	250
f_{livb}	Fraction Pu transferred from blood to liver	0.12
m_{liv}	Mass of liver (g)	3950
T_{liv}	Biological half time of Pu in liver (day)	30,000
Time	Time of slaughter after birth (day)	730

Table 3. Parameters and their values for the milk-cow submodel.

Parameters	Description	Value
WMILK	Weight of milk cow (kg)	650
PMILK	Daily production of milk (kg/day)	25
FAC	Energy required to produce one kg of milk (kcal)	1850
DIG_A	Digestibility factor for alfalfa	0.52
F_{alf}	Plowing depth in units of 5 cm	6
F_{milkb}	Fraction of Pu transferred from blood to milk	0.007
T_{milk}	Residence time of milk in cow (day)	0.75
I_{vd}	Daily ingestion of desert vegetation (g/day)	10,000
I_{va}	Daily ingestion of alfalfa (g/day)	15,000

Table 4. Parameters and their values for the inhalation and lung submodel for man.

Parameter	Description	Value
B_m	Respiration rate (m^3/day)	20
FR_i	Fraction of Pu in particle-size class	
	AMAD: 0.05, 0.1, 0.3, 0.5, 1.0,	0,0,0,1,
	2.0, 5.0 μm (simulation)	0,0,0
FR_i	Fraction of Pu in particle size classes	
	(sensitivity analysis)	all 0.143
$D_{3,i}$	Fraction of Pu in size class i deposited	.001,.008,.063,
	in nasopharyngeal (NP) region	.13,.29,.5,.77
$D_{4,i}$	Fraction of Pu in size class i deposited	.08,.08,.08,
	in tracheobronchial (TB) region	.08,.08,.08,.08
$D_{5,i}$	Fraction of Pu in size class i deposited	.59,.5,.36,
	in pulmonary (P) region (lung)	.31,.23,.17,.11
f_a	Fraction of Pu deposited in NP region that	
	is cleared to blood (compartment a)	.01
T_a^b	Biological half time of Pu in lung-model	
	compartment a (days)	.01
f_b	Fraction of Pu deposited in NP region	
	that is cleared to gut (compartment b)	.99
T_b^b	Biological half time of Pu in lung-model	
	compartment b (days)	.4
f_c	Fraction of Pu deposited in TB region	
	that is cleared to blood (compartment c)	.01
T_c^b	Biological half time of Pu in lung-model	
	compartment c (days)	.01

Table 4. (continued)

Parameter	Description	Value
f_d	Fraction of Pu deposited in TB region that is cleared to gut (compartment d)	.99
T_d^b	Biological half time of Pu in lung-model compartment d (days)	.2
f_e	Fraction of Pu deposited in lung that is cleared to blood (compartment e)	.05
T_e^b	Biological half time of Pu in lung-model compartment e (days)	500
f_f	Fraction of Pu deposited in lung that is cleared to gut quickly (compartment f)	.4
T_f^b	Biological half time of Pu in lung-model compartment f (days)	1
f_g	Fraction of Pu deposited in lung that is cleared to gut slowly (compartment g)	.4
T_g^b	Biological half time of Pu in lung-model compartment g (days)	500
f_h	Fraction of Pu deposited in lung that is cleared to lymph (compartment h)	.15
T_h^b	Biological half time of Pu in lung-model compartment h (days)	500
f_i	Fraction of Pu transferred from lung to lymph compartment i to blood	.9

Table 4. (concluded)

Parameter	Description	Value
T_i^b	Biological half time of Pu in lymph (days)	1000
$T_{TB,fg}$	Residence time of Pu in TB region in transfer from lung to gut (days)	.0417
λ_A	Decay rate of Pu (day^{-1})	7.783×10^{-8}

Table 5. Parameters and their values for the ingestion submodel for man.

Parameter	Description	Value
I_1	Ingestion rate for accidental soil ingestion (g/day)	0.01
I_2	Ingestion rate for leafy (washed) vegetables (g/day)	81
I_3	Ingestion rate for other (peeled) vegetables (g/day)	222
I_4	Ingestion rate of beef muscle (g/day)	273
I_5	Ingestion rate of beef liver (g/day)	13
I_6	Ingestion rate of cow's milk (g/day)	436
Wash	Fraction Pu remaining after surface washing of vegetables	0.1
Peel	Fraction Pu remaining after peeling of vegetables	0.01

Table 6. Parameters and their values for the redistribution of Pu in man.

Parameter	Description	Value
T_{GIT}	Residence time of food in the GI tract (days)	0.75
f_j	Fraction of Pu transferred from gut to blood	3×10^{-5}
f_{BL}	Fraction of Pu transferred from blood to liver	.45
T_L	Biological half time of Pu in the liver (days)	14600
f_{BK}	Fraction of Pu transferred from blood to kidney	0.02
f_{BBN}	Fraction of Pu transferred from blood to bone	0.45
T_K	Biological half time of Pu in the kidneys (days)	32000
T_{BN}	Biological half time of Pu in the bone (days)	36500
f_{BTB}	Fraction of Pu transferred from blood to the total body	1
T_{TOTB}	Biological half time of Pu in the total body (days)	65000

Table 7. Parameters and their values for calculating the dose of man.

Parameter	Description	Value
ϵ_{GIT}	Effective energy absorbed in gut per disintegration (Mev/dis)	0.52
ϵ_{LUNG}	Effective energy absorbed in lung per disintegration (Mev/dis)	53
ϵ_{BON}	Effective energy absorbed in bone per disintegration (Mev/dis)	266
ϵ_{LIV}	Effective energy absorbed in liver per disintegration (Mev/dis)	53
ϵ_{KID}	Effective energy absorbed in kidney per disintegration (Mev/dis)	53
ϵ_{TOTB}	Effective energy absorbed in total body per disintegration (Mev/dis)	53
ϵ_{NP}	Effective energy absorbed in nasopharyngeal region per disintegration (Mev/dis)	53
ϵ_{TRB}	Effective energy absorbed in tracheobronchial region per disintegration (Mev/dis)	53
ϵ_{LYMP}	Effective energy absorbed in thoracic lymph nodes region per disintegration (Mev/dis)	53
m_{GIT}	Mass of the GI tract (g)	150
m_{LUNG}	Mass of the lung (g)	500
m_{BONE}	Mass of the bone (g)	7000
m_{LIV}	Mass of the liver (g)	1700
m_{KID}	Mass of the kidney (g)	300

Table 7. (concluded).

Parameter	Description	Value
m_{TOTB}	Mass of the total body (g)	70,000
m_{NP}	Mass of the nasopharyngeal region (g)	1.35
m_{TRB}	Mass of the tracheobronchial region (g)	400
m_{LYMP}	Mass of the thoracic lymph node (g)	15

Table 8. Sensitivity of lung dose to changes in parameters.

Parameter	Characterization	Sensitivity
Concentration in soil, C_s	Environmental	1.0
Mass loading factor for air, L_a	Environmental	1.0
Respiration rate for man, B_m	Physiological	1.0
Dose-rate factor for lung, ϵ_{lung}	Biophysical	1.0
Mass of lung, m_{lung}	Lung model	-0.91
Fraction deposited in 500-d lung compartment cleared to GI, f_g	Lung model	0.67
Residence time of above compartment, T_g^b	Lung model	0.64
Fraction of 0.05μ particles retained by lung, $D_{5,1}$	Lung model	0.26
Fraction of lung particles cleared to lymph nodes, f_h	Lung model	0.25
Residence time of above (lung) compartment, T_h^b	Lung model	0.24
Fraction of 0.1μ particles retained in lung, $D_{5,2}$	Lung model	0.22
Fraction of 0.3μ particles retained in lung, $D_{5,3}$	Lung model	0.16
Fraction of Pu in particle class 0.05μ, FR_1	Environmental	0.14
Fraction of 0.5μ particles retained in lung, $D_{5,4}$	Lung model	0.14
14 other parameters	Environmental (particle size) Lung model	>0.0 but $\leq$0.11
83 other parameters	Ecological (food chain), Lung model, Bone model, GI model, etc.	0.0

Table 9. Sensitivity of bone dose to changes in parameters.

Parameter	Characterization	Sensitivity
Concentration of Pu in soil, C_s	Environmental	1.0
Transfer coefficient blood to bone, f_{BBN}	Bone model	1.0
Dose factor for bone, ϵ_{BON}	Biophysical	1.0
Mass loading factor for air, L_a	Environmental	0.95
Respiration rate for man, B_m	Physiological	0.95
Mass of bone, m_{BON}	Bone model	-0.91
Fraction deposited in lung cleared to lymph, f_h	Lung model	0.62
Fraction of Pu cleared to lymph from lung, f_i	Lung model	0.62
Fraction deposited in lung cleared to blood, f_e	Lung model	0.27
Fraction of 0.05μ particles retained in lung, $D_{5,1}$	Lung model	0.23
Fraction of 0.1μ particles retained in lung, $D_{5,2}$	Lung model	0.20
Fraction of 0.3μ particles retained in lung, $D_{5,3}$	Lung model	0.14
Fraction of 0.5μm particles retained in lung, $D_{5,4}$	Lung model	0.12
All others	Environmental	$\leq$ 0.10
	Lung model	
	Bone model	
Concentration factor for plants, CF_v	Environmental	0.048
Ingestion rate of leafy vegetables, I_2	Environmental	0.036
Ingestion rate of other vegetables, I_3	Environmental	0.0099
Accidental ingestion rate of soil by man, I_1	Environmental	0.0027
Ingestion rate of beef liver, I_5	Environmental	0.0020
Ingestion of beef muscle, I_4	Environmental	0.00068
Ingestion rate of milk, I_6	Environmental	$\leq 5 \times 10^{-6}$

Table 10. Sensitivity of liver dose to changes in parameters.

Parameter	Characterization	Sensitivity
Concentration Pu in soil, C_s	Environmental	1.0
Transfer coefficient blood to liver, f_{BL}	Liver model	1.0
Dose factor for liver, ϵ_{LIV}	Biophysical	1.0
Mass loading factor for air, L_a	Environmental	0.95
Respiration rate for man, B_m	Physiological	0.95
Mass of liver, m_{LIV}	Dose model	-0.91
Fraction deposited in lung cleared to lymph, f_h	Lung model	0.62
Fraction of Pu cleared to lymph from lung, f_i	Lung model	0.62
Fraction deposited in lung cleared to blood, f_e	Lung model	0.27
Fraction 0.05μ particles retained by lung, $D_{5,1}$	Lung model	0.23
Biological half time of Pu in liver, T_L	Liver model	0.22
Fraction of 0.1μ particles retained in lung, $D_{5,2}$	Lung model	0.20
Fraction of 0.3μ particles retained in lung, $D_{5,3}$	Lung model	0.14
Fraction of 0.5μ particles retained in lung, $D_{5,4}$	Lung model	0.12
Fraction of Pu in particle class 0.05μ, FR_1	Environmental	0.11
21 parameters	Environmental (food chain) but	$\geq$0.01 $\leq$0.1
36 parameters	Vegetable and cattle models but	$\geq$0.00001 $\leq$0.01
15 parameters	Lung, bone, etc. models	>0 but $<0.5 \times 10^{-5}$
24 parameters	Bone, kidney, etc. models	0.0

Table 10. (concluded).

Parameter	Characterization	Sensitivity
Ingestion rate of washed vegetables, I_2	Environmental	0.036
Ingestion rate of peeled vegetables, I_3	Environmental	0.0098
Accidental ingestion of soil, I_1	Environmental	0.0027
Ingestion rate of beef liver, I_5	Environmental	0.0020
Ingestion rate of beef muscle, I_4	Environmental	0.00067

Table 11. Sensitivity of GI tract dose to changes in parameters.

Parameter	Characterization	Sensitivity
Concentration in soil, C_s	Environmental	1.0
Residence time in GI tract, T_{GIT}	GI model	1.0
Dose-rate factor for GI tract, ϵ_{GIT}	Biophysical	1.0
Concentration factor for vegetation, CF_v	Environmental	0.93
Mass of GI tract, m_{GIT}	GI model	-0.91
Soil mixing depth by cultivation, F_{alf}	Environmental	-0.81
Fraction Pu retained after washing leafy vegetables, Wash	Environmental	0.70
Ingestion rate of leafy vegetables, I_2	Environmental	0.70
Fraction Pu retained after peeling vegetables, Peel	Environmental	0.19
Ingestion rate of other vegetables, I_3	Environmental	0.19
Power parameter for calculating cattle ingestion, CF_2	Cow model	0.18
Accidental ingestion rate of soil by man, I_1	Environmental	0.052
55 other parameters	Cattle models, lung model, environmental (food chain)	>0.0 but <0.052
including: Ingestion rate of beef liver, I_5	Environmental	0.038
Ingestion rate of beef muscle, I_4	Environmental	0.013
Ingestion rate of milk, I_6	Environmental	0.00003
44 other parameters	Bone, lung, liver model, etc.	0.0

Table 12. Sensitivity of organ dose to pathways.

Pathway/parameter	Organ sensitivity							
	GIT	URT	Lung	Lymph	Liver	Kidney	Bone	Total body
Inhalation								
L_a, mass loading factor for air	0.006	1.0	1.0	1.0	0.949	0.949	0.949	0.948
Ingestion (analysis at intake)								
I_1 accidental ingestion of soil by man	0.052	0.0	0.0	0.0	.0027	.0027	.0027	.0027
I_2 leafy (washed) vegetables	0.70	0.0	0.0	0.0	.036	.036	.036	.036
I_3 other (peeled) vegetables	.19	0.0	0.0	0.0	.0098	.0099	.0099	.010
I_4 beef muscle	.013	0.0	0.0	0.0	.00067	.00068	.00068	.00068
I_5 beef liver	.038	0.0	0.0	0.0	.0020	.0020	.0020	.0020
I_6 milk	.00003	0.0	0.0	0.0	0.0	0.0	0.0	0.0
Ingestion (analysis at soil source)								
Through vegetation, CFV, concentration factor for plants	0.927	0.0	0.0	0.0	.047	.048	.048	.048
Accidental soil ingestion by man, I_1	.052	0.0	0.0	0.0	.0027	.0027	.0027	.0027
Accidental soil ingestion by cattle, I_s	0.015	0.0	0.0	0.0	0.00076	0.00077	0.00077	0.00078

Table 13. Relative spread of distribution of doses in uncertainty analysis by organ.

Variable	σ/m
All parameters	0.03
GI tract dose	0.08
Upper respiratory tract dose	0.08
Lung dose	0.08
Lymph dose	0.11
Liver dose	0.08
Kidney dose	0.08
Bose dose	0.08
Total body dose	0.08

FIGURE CAPTIONS

Figure 1. Schematic diagram showing compartments of major submodels of the NAEG model. Transfers of Pu between compartments are shown by solid arrows. The man submodel is surrounded by a dashed line.

Figure 2. Schematic diagram of the beef-cattle submodel. Internal transfers between cattle organs are shown within dashed line.

Figure 3. Schematic diagram of the milk-cow submodel showing Pu pathways.

Figure 4. Schematic diagram of the man submodel. Inputs are inhalation (A_m) and ingestion (H_m) of Pu. Solid arrows show movement of Pu between organs.

Figure 5. Cumulative dose to man in four organs for a 50-year simulation of a constant exposure to soil containing 1 pCi of ^{239}Pu/g.

Figure 6. Cumulative dose to all organs calculated in the NAEG model. Simulation is for a 50-year exposure to environmental values in Tables 1 through 7.

Figure 7. Histograms of distribution of organ doses for 1000 simulations of 50-year dose where the parameters were allowed to vary independently between simulations.

Figure 8. Log transformed organ doses plotted on probability scales for the distributions shown in Fig. 7.

Figure 9. Organ doses (untransformed) plotted on probability scales (probits) for the distributions shown in Fig. 7.

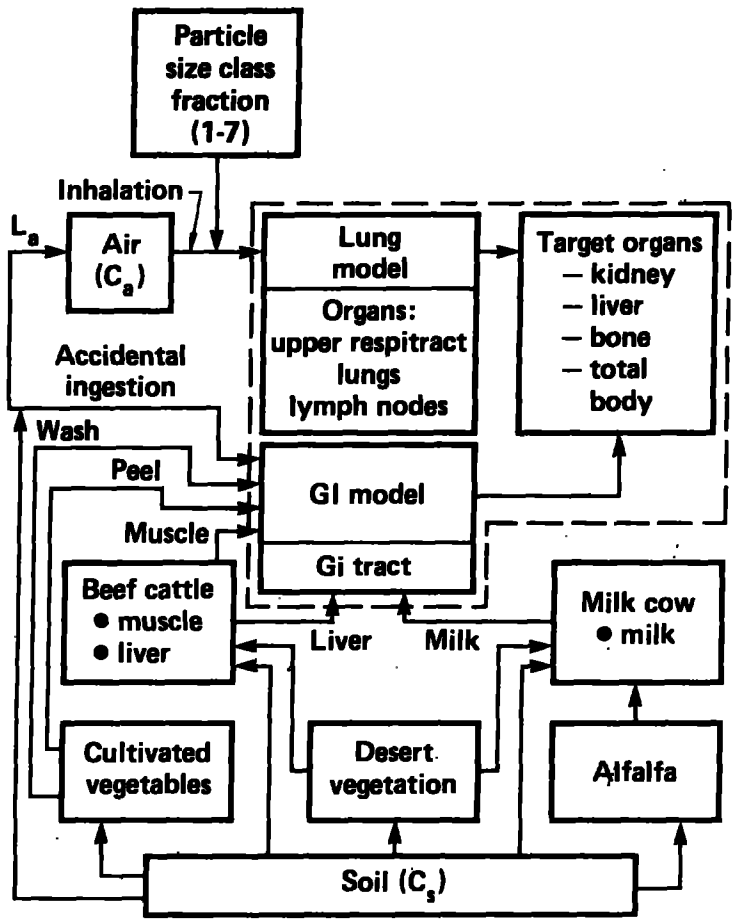
Particle size class fraction (1-7)
Inhalation
L_a
Air (C_a)
Lung model
Organs: upper respitract lungs lymph nodes
Target organs
– kidney
– liver
– bone
– total body
Accidental ingestion
Wash
Peel
Muscle
GI model
Gi tract
Beef cattle
• muscle
• liver
Liver
Milk
Milk cow
• milk
Cultivated vegetables
Desert vegetation
Alfalfa
Soil (C_s)

Figure 1

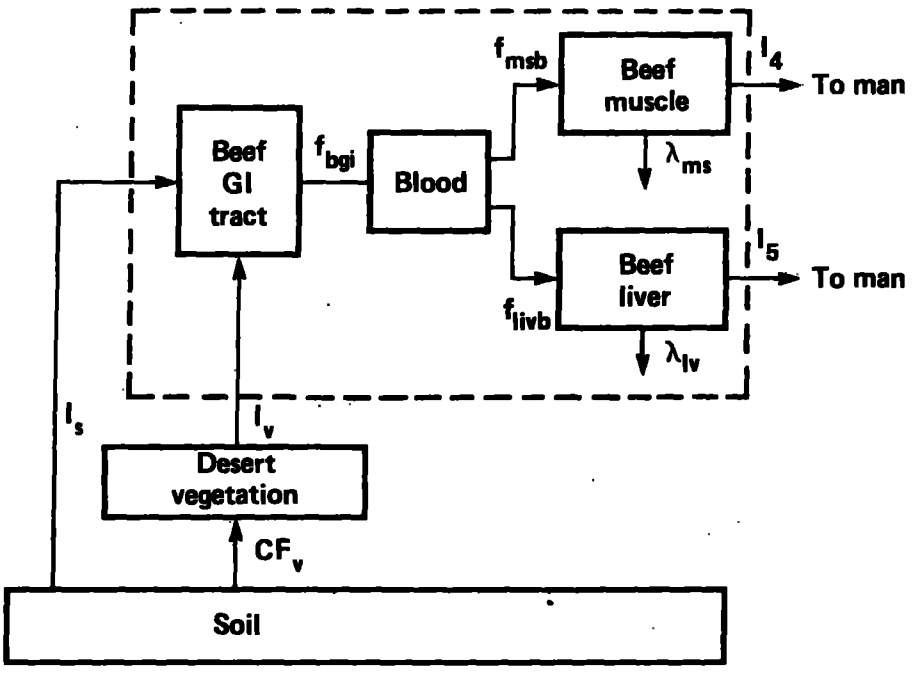
Beef GI tract
f_{bgi}
Blood
f_{msb}
Beef muscle
I_4
To man
λ_{ms}
f_{livb}
Beef liver
I_5
To man
λ_{lv}
I_s
I_v
Desert vegetation
CF_v
Soil

Figure 2

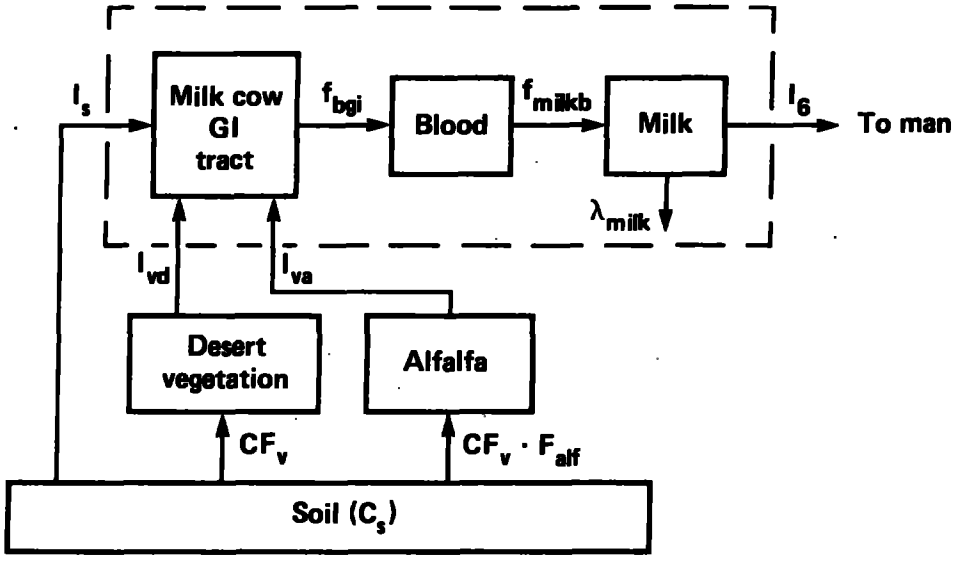
I_s
Milk cow GI tract
f_{bgi}
Blood
f_{milkb}
Milk
I_6
To man
λ_{milk}
I_{vd}
I_{va}
Desert vegetation
Alfalfa
CF_v
$CF_v \cdot F_{alf}$
Soil (C_s)

Figure 3

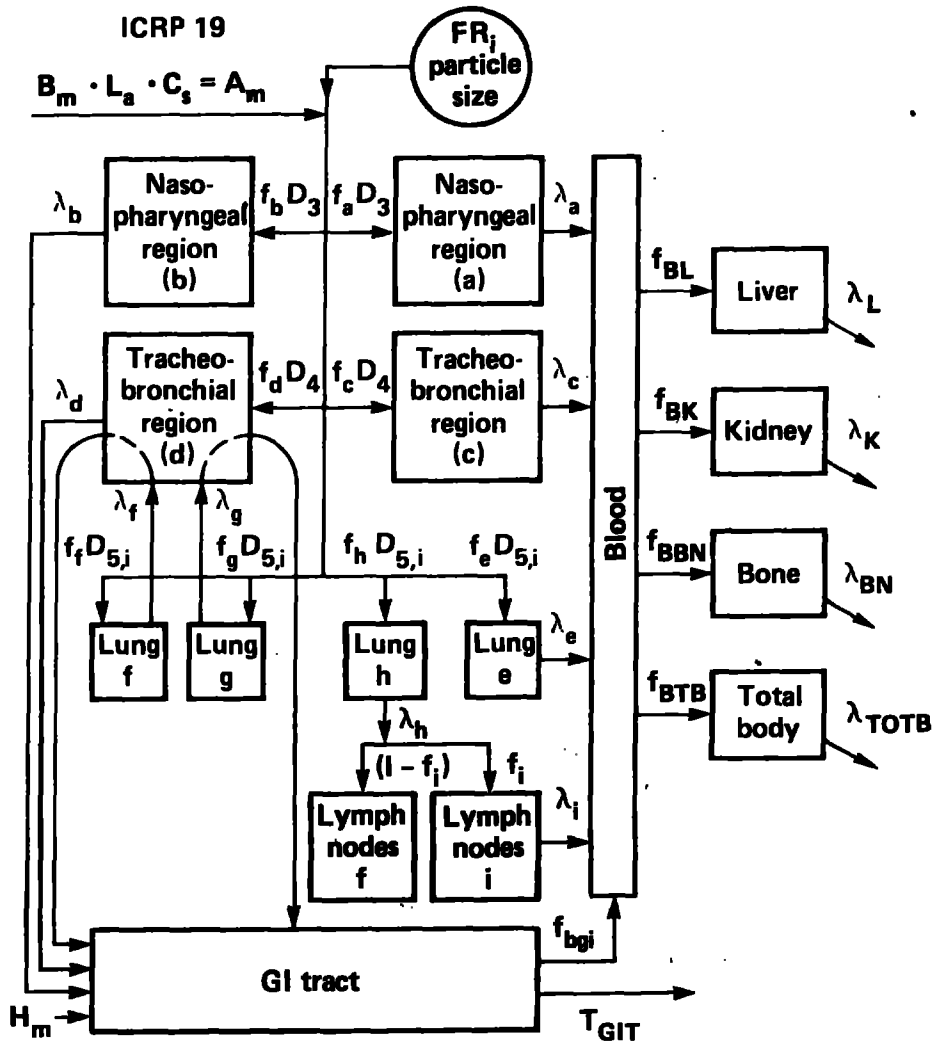
ICRP 19
$B_m \cdot L_a \cdot C_s = A_m$
FR_i particle size
Naso-pharyngeal region (b)
Naso-pharyngeal region (a)
Tracheo-bronchial region (d)
Tracheo-bronchial region (c)
Lung f
Lung g
Lung h
Lung e
Lymph nodes f
Lymph nodes i
Blood
Liver
Kidney
Bone
Total body
GI tract
λ_b
$f_b D_3$
$f_a D_3$
λ_a
λ_d
$f_d D_4$
$f_c D_4$
λ_c
λ_f
λ_g
$f_f D_{5,i}$
$f_g D_{5,i}$
$f_h D_{5,i}$
$f_e D_{5,i}$
λ_e
λ_h
$(1 - f_i)$
f_i
λ_i
f_{BL}
λ_L
f_{BK}
λ_K
f_{BBN}
λ_{BN}
f_{BTB}
λ_{TOTB}
f_{bgi}
H_m
T_{GIT}

Figure 4

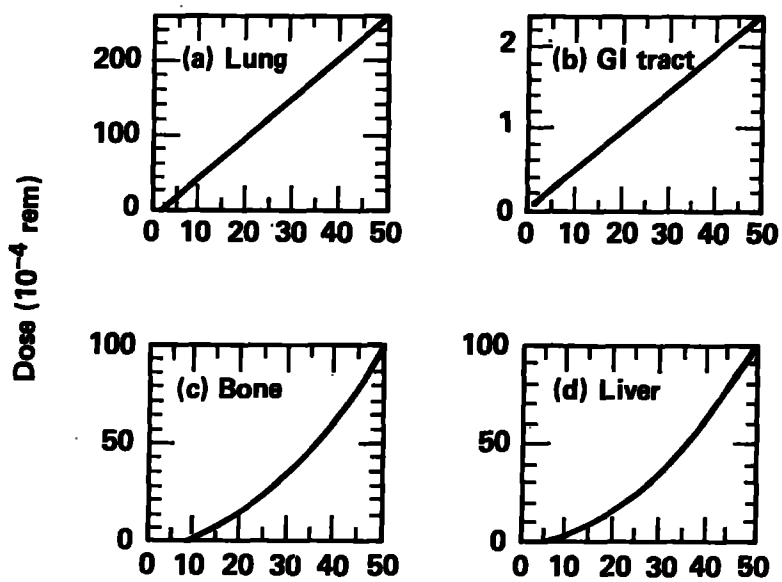
Dose (10^{-4} rem)
(a) Lung
200
100
0
0 10 20 30 40 50
(b) GI tract
2
1
0
0 10 20 30 40 50
(c) Bone
100
50
0
0 10 20 30 40 50
(d) Liver
100
50
0
0 10 20 30 40 50

Figure 5

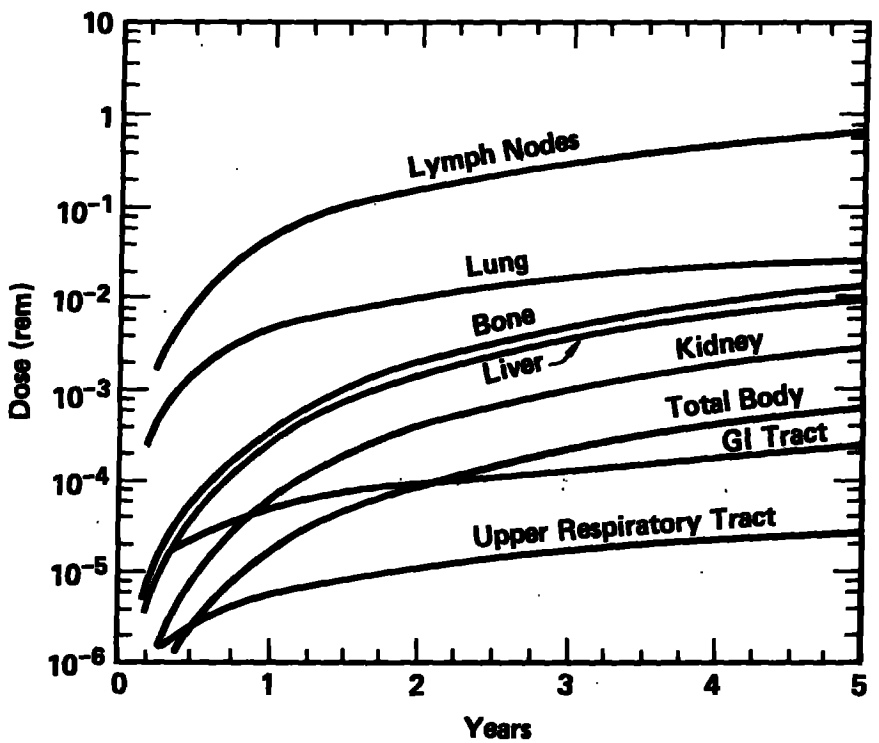
10
1
10^{-1}
10^{-2}
10^{-3}
10^{-4}
10^{-5}
10^{-6}
Dose (rem)
Lymph Nodes
Lung
Bone
Liver
Kidney
Total Body
GI Tract
Upper Respiratory Tract
0
1
2
3
4
5
Years

Figure 6

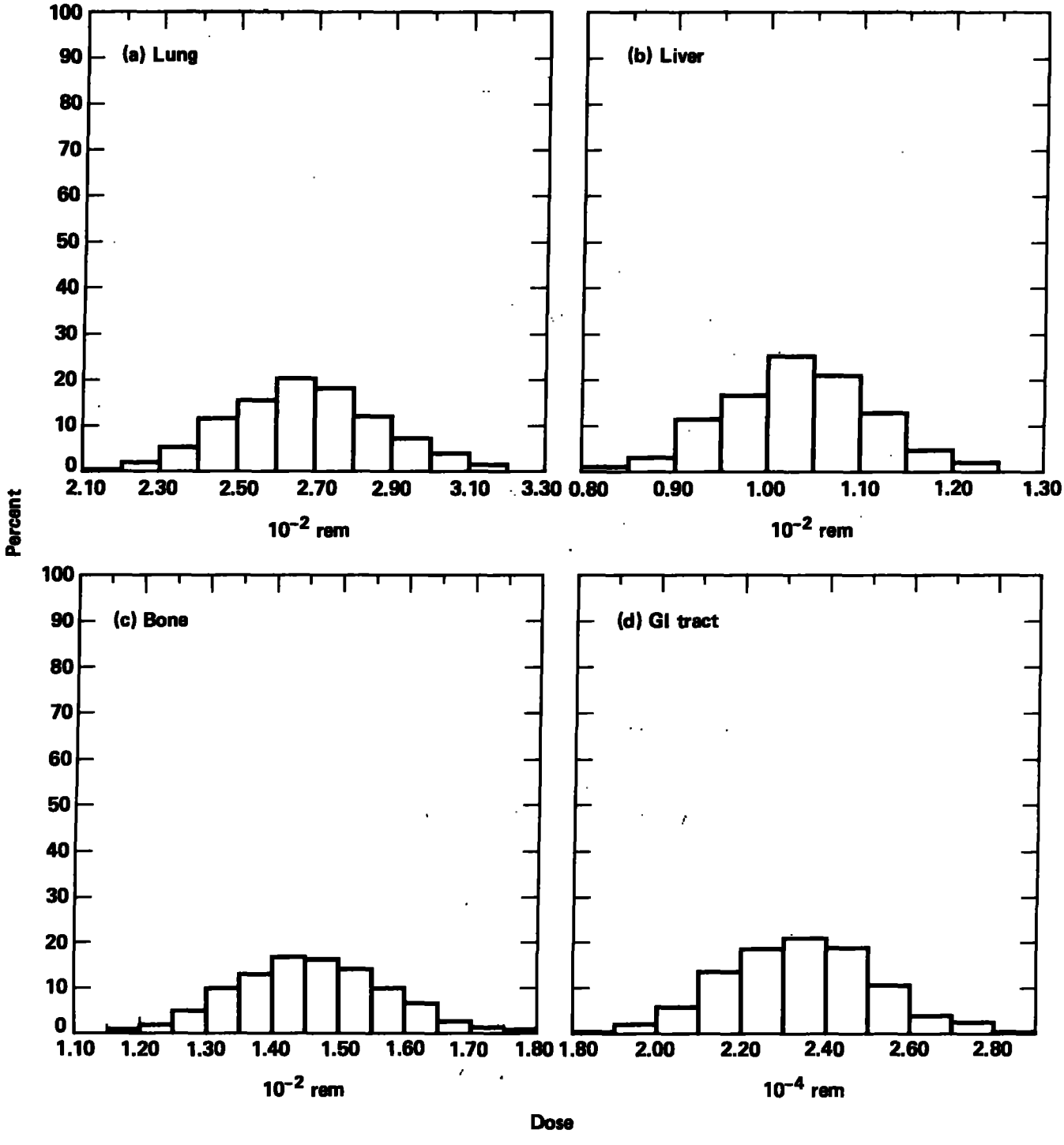
(a) Lung
(b) Liver
(c) Bone
(d) GI tract
Percent
100
90
80
70
60
50
40
30
20
10
0
2.10 2.30 2.50 2.70 2.90 3.10 3.30
0.80 0.90 1.00 1.10 1.20 1.30
1.10 1.20 1.30 1.40 1.50 1.60 1.70 1.80
1.80 2.00 2.20 2.40 2.60 2.80
10^{-2} rem
10^{-2} rem
10^{-2} rem
10^{-4} rem
Dose

Figure 7

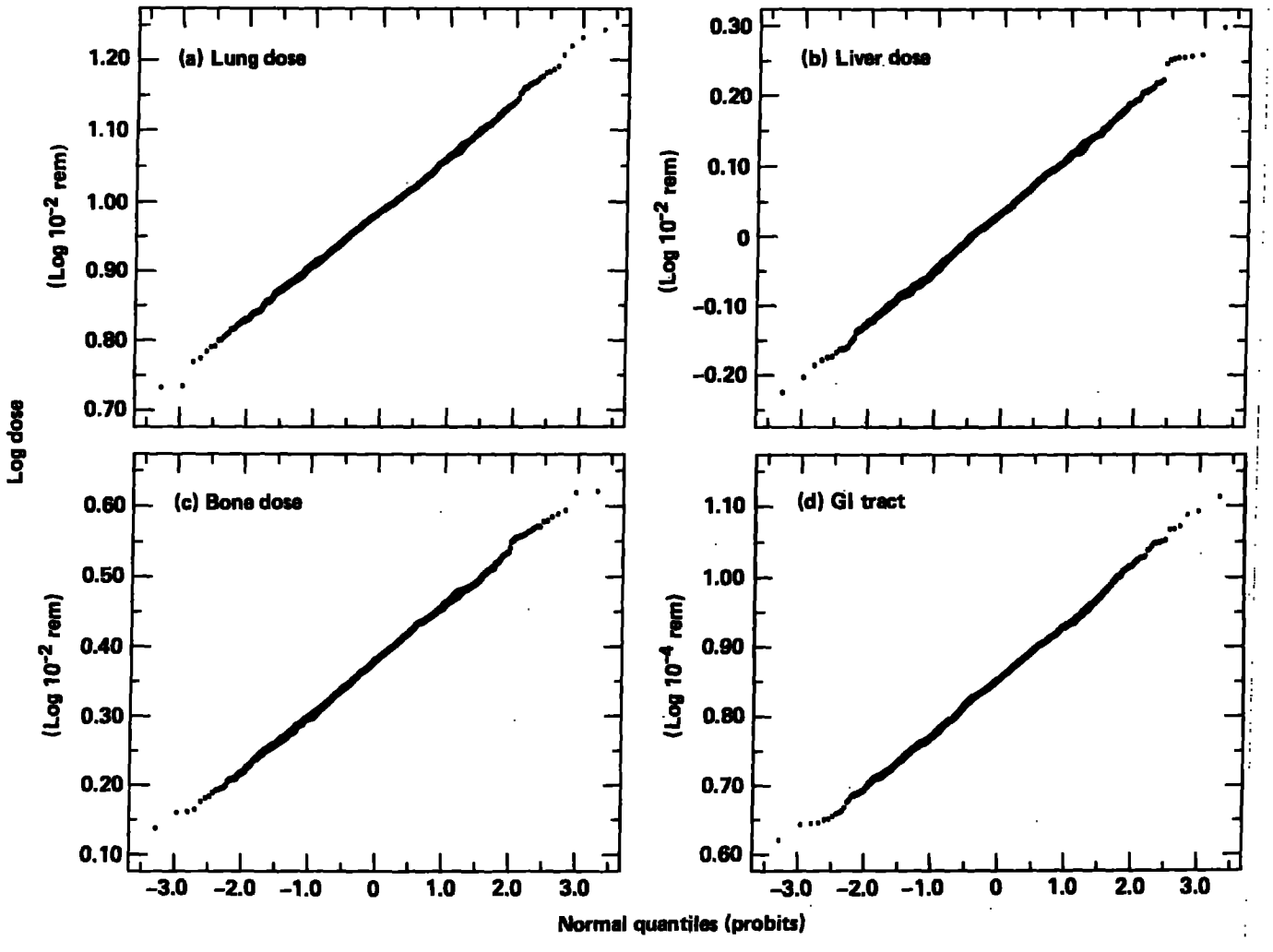
(a) Lung dose
(b) Liver dose
(c) Bone dose
(d) GI tract
Log dose
(Log 10⁻² rem)
(Log 10⁻² rem)
(Log 10⁻² rem)
(Log 10⁻⁴ rem)
1.20
1.10
1.00
0.90
0.80
0.70
0.30
0.20
0.10
0
-0.10
-0.20
0.60
0.50
0.40
0.30
0.20
0.10
1.10
1.00
0.90
0.80
0.70
0.60
-3.0
-2.0
-1.0
0
1.0
2.0
3.0
Normal quantiles (probits)

Figure 8

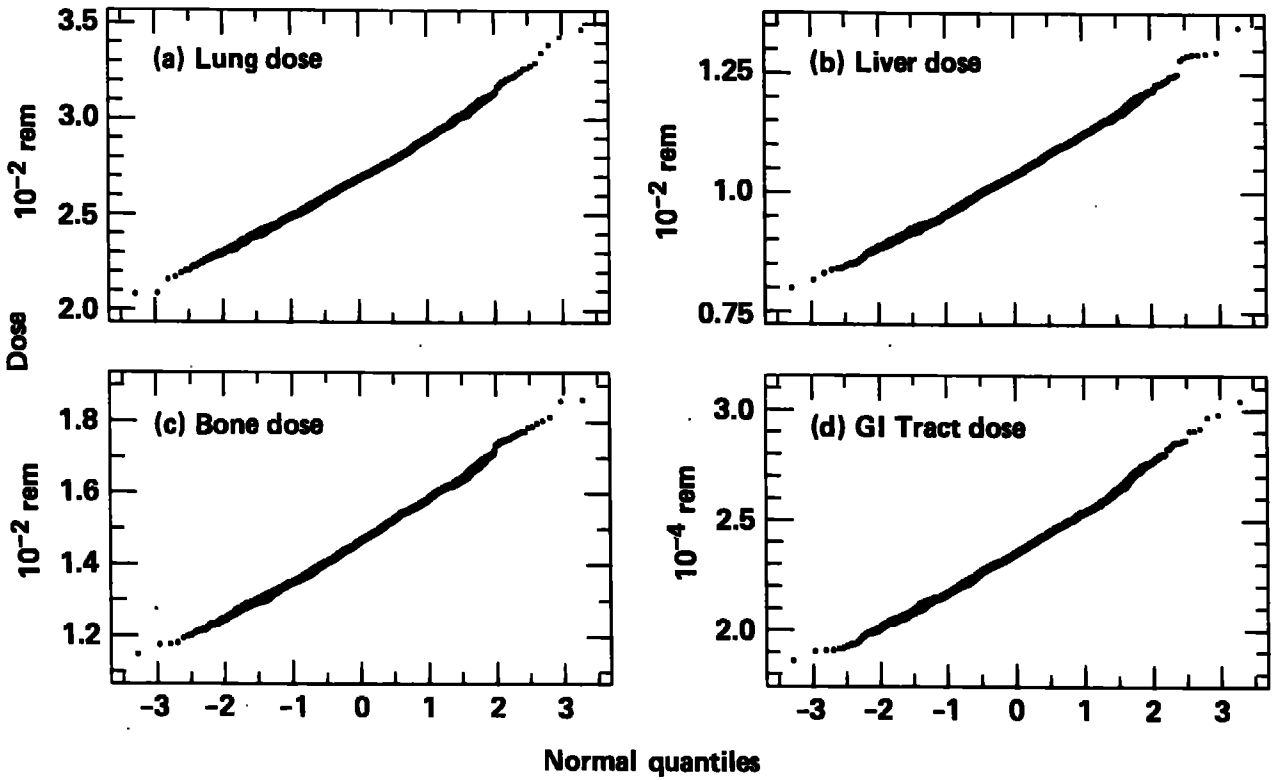
(a) Lung dose
(b) Liver dose
(c) Bone dose
(d) GI Tract dose
Dose
10^{-2} rem
10^{-2} rem
10^{-2} rem
10^{-4} rem
3.5
3.0
2.5
2.0
1.25
1.0
0.75
1.8
1.6
1.4
1.2
3.0
2.5
2.0
-3 -2 -1 0 1 2 3
Normal quantiles

Figure 9